Behavioral/Systems/Cognitive

Cholinergic Inhibition of Neocortical Pyramidal Neurons

Allan T. Gulledge[1,2] **and Greg J. Stuart**[1]

[1]Division of Neuroscience, John Curtin School of Medical Research, Australian National University, Canberra, Australian Capital Territory, 0200, Australia, and [2]Division of Cerebral Circuitry, National Institute for Physiological Sciences, Okazaki, Aichi 444-8787, Japan

Acetylcholine (ACh) is a central neurotransmitter critical for normal cognitive function. Here we show that transient muscarinic acetylcholine receptor activation directly inhibits neocortical layer 5 pyramidal neurons. Using whole-cell and cell-attached recordings from neurons in slices of rat somatosensory cortex, we demonstrate that transient activation of M_1-type muscarinic receptors induces calcium release from IP_3-sensitive intracellular calcium stores and subsequent activation of an apamin-sensitive, SK-type calcium-activated potassium conductance. ACh-induced hyperpolarizing responses were blocked by atropine and pirenzepine but not by methoctramine or GABA receptor antagonists (picrotoxin, SR 95531 [2-(3-carboxypropyl)-3-amino-6-(4-methoxyphenyl)pyridazinium bromide], and CGP 55845 [(2*S*)-3-[[(15)-1-(3,4-dichlorophenyl)ethyl]amino-2-hydroxypropyl](phenylmethyl)phosphinic acid]). Responses were associated with a 31 ± 5% increase in membrane conductance, had a reversal potential of −93 ± 1 mV, and were eliminated after internal calcium chelation with BAPTA, blockade of IP_3 receptors, or extracellular application of cadmium but not by sodium channel blockade with tetrodotoxin. Calcium-imaging experiments demonstrated that ACh-induced hyperpolarizing, but not depolarizing, responses were correlated with large increases in intracellular calcium. Surprisingly, transient increases in muscarinic receptor activation were capable of generating hyperpolarizing responses even during periods of tonic muscarinic activation sufficient to depolarize neurons to action potential threshold. Furthermore, eserine, an acetylcholinesterase inhibitor similar to those used therapeutically in the treatment of Alzheimer's disease, disproportionately enhanced the excitatory actions of acetylcholine while reducing the ability of acetylcholine to generate inhibitory responses during repeated applications of ACh. These data demonstrate that acetylcholine can directly inhibit the output of neocortical pyramidal neurons.

Key words: **neocortex; acetylcholine; muscarinic receptor; pyramidal neuron; SK channel; calcium imaging**

Introduction

Acetylcholine (ACh) is an important neurotransmitter critical for learning and memory (Hagan and Morris, 1988), and loss of cholinergic function contributes to the profound learning impairments and memory deficits associated with age-related dementia and Alzheimer's disease (Bartus et al., 1982; Kasa et al., 1997). Evidence supporting a role for ACh in cognitive processes includes the findings that muscarinic acetylcholine receptor (mAChR) antagonists impair memory in animals (Buresova et al., 1986) and humans (Drachman and Leavitt, 1974), and that mAChR activation facilitates the long-term synaptic plasticity thought to be the physiological substrate of learning and memory (Blitzer et al., 1990; Burgard and Sarvey, 1990; Hasselmo and Barkai, 1995; Ovsepian et al., 2004).

A number of studies have examined the influence of ACh and cholinergic agonists on pyramidal neuron excitability in the cortex. Studies using intracellular current-clamp recordings have generally found mAChR activation to be excitatory, producing depolarizing responses in neurons and facilitating action potential generation (Krnjevic et al., 1971; McCormick and Prince, 1985, 1986; Schwindt et al., 1988; Halliwell, 1989; Andrade, 1991; Metherate et al., 1992; Wang and McCormick, 1993; Gloveli et al., 1999; Egorov et al., 2002, 2003). These direct excitatory effects have been attributed to mAChR-mediated inhibition of potassium conductances (Krnjevic et al., 1971; Schwindt et al., 1988; McCormick and Williamson, 1989; McCormick, 1990; Nishikawa et al., 1994), although more recent data suggest that ACh may also increase activation of a nonselective cation conductance (Andrade, 1991; Haj-Dahmane and Andrade, 1996, 1998; Klink and Alonso, 1997; Shalinsky et al., 2002; Egorov et al., 2003).

In a minority of studies, inhibitory actions of ACh on neocortical pyramidal neurons have been reported (McCormick and Prince, 1985, 1986; Halliwell, 1989; Müller and Singer, 1989; Bandrowski et al., 2001; Yamamoto et al., 2002). Experiments conducted *in vitro* found that pressure applications of high concentrations of exogenous ACh (1–50 mM) can hyperpolarize pyramidal neurons (McCormick and Prince, 1985, 1986). Because responses were found to be sensitive to classical inhibitors of synaptic transmission [low external Ca^{2+} or tetrodotoxin (TTX)] and to blockers of $GABA_A$ channels (picrotoxin or bicuculline), the inhibitory actions of ACh were attributed to increased GABA transmission after mAChR-mediated excitation of interneurons (McCormick and Prince, 1985, 1986). Similar observations suggested that a GABAergic mechanism was responsible for the mAChR-mediated inhibition reported by Bandrowski et al. (2001) in rat auditory cortex *in vitro* and by Müller and Singer (1989) in cat visual cortex *in vivo*.

Received June 30, 2005; revised Sept. 27, 2005; accepted Oct. 1, 2005.

This work was supported by the National Health and Medical Research Council of Australia.

Correspondence should be addressed to Allan T. Gulledge, Division of Cerebral Circuitry, National Institute for Physiological Sciences, 5-1 Higashiyama, Myodaiji, Okazaki, Aichi 444-8787, Japan. E-mail: allan@nips.ac.jp.

DOI:10.1523/JNEUROSCI.2697-05.2005

 0270-6474/05/2510308-13$15.00/0

Because these previous studies typically used high concentrations of muscarinic agonists (1–100 mM) (Krnjevic et al., 1971; McCormick and Prince, 1985, 1986; Schwindt et al., 1988; McCormick and Williamson, 1989; Müller and Singer, 1989; Wang and McCormick, 1993; Gloveli et al., 1999; Egorov et al., 2002, 2003) or prolonged, tonic mAChR stimulation (Schwindt et al., 1988; Halliwell, 1989; Yamamoto et al., 2002), the resulting data do not describe the actions of transient mAChR activation, as is likely to happen during synaptic release of ACh (Metherate et al., 1992; Bandrowski et al., 2001). In this study, we use rapid and focal application of relatively low concentrations of mAChR agonists to show that transient mAChR activation generates strong and direct inhibition of neocortical pyramidal neurons by inducing calcium release from internal stores and subsequent activation of an SK-type calcium-activated potassium conductance.

Materials and Methods

Recordings were made from visually identified layer 5 pyramidal neurons in coronal brain slices (300 μm thick) of somatosensory cortex prepared from 3- to 5-week-old or 10-week-old Wistar rats according to methods approved by the Australian National University. Slices were perfused with a solution [artificial CSF (aCSF)] containing the following (in mM): 125 NaCl, 25 $NaHCO_3$, 3 KCl, 1.25 NaH_2PO_4, 2 $CaCl_2$, 1 $MgCl_2$, and 25 glucose (at 35°C, bubbled with 95% O_2/5% CO_2). Whole-cell recording pipettes (5–7 MΩ) contained the following (in mM): 135 K-gluconate or K-methylsulfate, 7 NaCl, 2 $MgCl_2$, 10 HEPES, 2 Na_2ATP, and 0.3 NaGTP, pH 7.2 with KOH. No significant differences were observed in cholinergic responses recorded in cells recorded with K-gluconate or K-methylsulfate solutions. For extracellular recordings, recording pipettes were filled with regular aCSF and placed near the axon initial segment. Data were acquired using a BVC-700 amplifier (Dagan, Minneapolis, MN) and a Macintosh computer (Apple Computers, Cupertino, CA) running AxoGraph 4.9 (Molecular Devices, Union City, CA). Whole-cell series resistance was generally between 10 and 25 MΩ and was maximally compensated. Membrane potentials were corrected for the liquid junction potential (−12 mV for K-gluconate pipettes; −8 mV for K-MSO_4 pipettes). ACh-mediated hyperpolarizations were measured relative to the resting membrane potential immediately before drug application. The magnitude of ACh-induced hyperpolarizations during firing was measured from the minimum membrane potential achieved during interspike afterhyperpolarizations. For transient activation of mAChR agonists, patch pipettes were filled with 100 μM carbachol or ACh dissolved in aCSF, connected to a Picospritzer 3 (Parker Instrumentation, Chicago, IL), and brief applications of carbachol or ACh were applied close to the soma of recorded neurons (within 20 μm) using a pressure of 10 psi, unless otherwise indicated. To estimate the time course of solution exchange, 20 ms applications of intracellular pipette saline were delivered to neurons voltage clamped at −70 mV. In these control experiments, the 10–90% rise time of the generated inward currents was 12 ± 1 ms ($n = 3$). All ACh and carbachol applications to a given neuron were generated with the puff pipette positioned at the same location and using the same application duration, unless otherwise indicated. During bath application, drugs were washed in for 5 min before recording the effect of drug application and subsequently washed out up to 0.5 h. In the absence of pharmacological manipulations, responses to repeated focal ACh applications did not change during the duration of whole-cell recordings (up to 1 h) when interleaved by 5 s somatic depolarizations sufficient to generate action potential firing (data not shown). Drugs were obtained from Sigma (St. Louis, MO). $GABA_A$ receptor antagonists were coapplied with kynurenic acid (2 mM). For imaging experiments, cells were filled with 100 μM Oregon Green BAPTA-6F (OGB6F) (Invitrogen, Carlsbad, CA), and line scans (10 or 100 Hz temporal resolution) were made across the longitudinal axis of the soma using a confocal microscope (LSM 510; Zeiss, Oberkochen, Germany). Raw data were background subtracted, and the change in florescence relative to the resting fluorescence ($\Delta F/F$) was calculated over a 400 ms baseline period before ACh application. Data are presented as mean ± SEM. Statistical analysis used either the Student's *t* test (two tailed, paired or unpaired) or an ANOVA with a Tukey's *post hoc* test, for paired or unpaired data, as appropriate.

Results

Transient muscarinic receptor activation hyperpolarizes cortical pyramidal neurons

To examine the effect of transient mAChR activation, we focally applied ACh (100 μM) or carbachol (100 μM) near the soma of visually identified layer 5 pyramidal neurons (Fig. 1*A*). In all cells tested (>200), transient mAChR activation produced a delayed hyperpolarizing response from rest (Fig. 1*B*,*C*). Hyperpolarizing responses to 1-s-long applications of ACh (mean amplitude, −4.6 ± 0.5 mV; $n = 21$) or carbachol (mean amplitude, −4.8 ± 0.3 mV; $n = 30$) were not significantly different ($p = 0.6$), and data were therefore pooled. A more detailed comparison of hyperpolarizing responses to 1-s-long ACh and carbachol applications is presented in Table 1. For the combined dataset ($n = 51$), ACh or carbachol application (1 s) produced a biphasic response consisting of a delayed hyperpolarization followed by, or superimposed on, a slower depolarization. Hyperpolarizing responses had a mean latency of 344 ± 19 ms, a rise time of 208 ± 19 ms, an amplitude of −4.7 ± 0.3 mV, and half-widths of 568 ± 55 ms ($n = 51$). Two methods were used to confirm that hyperpolarizing responses to ACh or carbachol application were attributable to mAChR activation. First, to test that focal applications themselves do not induce hyperpolarizations, normal aCSF was focally applied to four neurons for 1 s periods. No significant change in membrane potential was observed in these cells (mean change in membrane potential during application of aCSF alone was −0.6 ± 0.2 mV; $n = 4$; $p = 0.2$; data not shown). Second, bath application of the muscarinic receptor antagonist atropine (10 μM) completely and irreversibly blocked hyperpolarizing responses in six of six neurons tested (Fig. 1*D*). In baseline conditions, carbachol application (1 s) generated responses of −3.4 ± 0.6 mV. After bath application of atropine (5 min), the mean change in membrane potential at a time corresponding to the peak of the hyperpolarization in baseline conditions was +0.2 ± 0.2 mV ($n = 6$; $p < 0.01$).

The biphasic response to transient mAChR activation described above contrasts with the depolarizing responses typically observed during tonic mAChR activation (Schwindt et al., 1988; Halliwell, 1989; Haj-Dahmane and Andrade, 1996). To determine the relationship between the duration of mAChR activation and the peak amplitude of hyperpolarizing and depolarizing responses, ACh was applied to a separate group of neurons for durations ranging from 5 to 1000 ms (Fig. 1*E*). The resulting "duration–response" curves for the hyperpolarizing and depolarizing components of the response were fit with exponential functions (Fig. 1*F*). This experiment indicated that hyperpolarizing and depolarizing responses reached steady state during ACh applications of <1 s duration. Exponential fits to these data demonstrate that, relative to hyperpolarizing responses ($\tau = 19 \pm 2$ ms), depolarizing responses ($\tau = 139 \pm 37$ ms) require approximately seven times longer periods of ACh exposure to generate maximum response amplitude ($n = 10$; $p < 0.05$). These data suggest that briefer periods of mAChR activation will favor the generation of hyperpolarizing responses over depolarization.

To determine whether hyperpolarizing responses to transient mAChR activation is specific to neurons from younger (3- to 5-week-old) animals, we focally applied ACh (50 ms) to pyramidal neurons in slices obtained from 10-week-old rats. As was observed in neurons from younger animals, transient mAChR

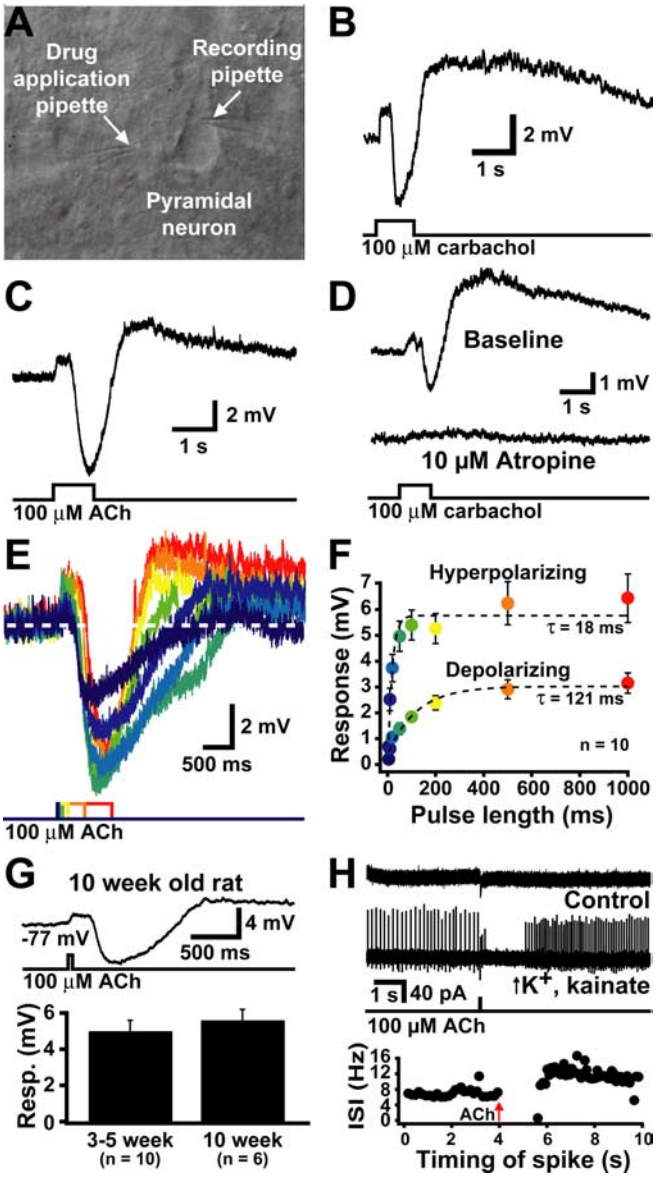

Figure 1. Transient muscarinic receptor activation hyperpolarizes cortical pyramidal neurons. ***A***, Image of experimental setup showing a layer 5 pyramidal neuron and the position of recording and drug-delivery pipettes. ***B–D***, Focal applications of carbachol (***B***) or acetylcholine (***C***) produce biphasic, hyperpolarizing and depolarizing, responses that are atropine sensitive (***D***). ***E***, Superimposed responses of a layer 5 pyramidal neuron to ACh applications of varying duration (5, 10, 20, 50, 100, 200, 500, and 1000 ms). ***F***, Plot of the mean peak hyperpolarizing and depolarizing responses produced by variable durations of ACh exposure ($n = 10$). Dashed lines indicate exponential fits to the averaged data from 10 neurons. The time constants of the averaged data were 18 ms for hyperpolarizing responses and 121 ms for depolarizing responses. ***G***, Hyperpolarizing responses to ACh (50 ms) recorded in pyramidal neurons in somatosensory slices from adult (10-week-old) rats (top), and a summary graph comparing responses in younger and older animals (bottom). ***H***, Extracellular recordings of responses to focal ACh application (20 ms) in a neuron before and after exposure to increased extracellular potassium (6 mM) and kainate (200 nM). Below is a plot of the instantaneous spike frequency (ISI) for this neuron showing the ACh-induced inhibition.

activation produced delayed and long-lasting hyperpolarizing responses in neurons from fully mature animals (Fig. 1*G*). The mean amplitude of hyperpolarization produced by ACh application in neurons from 10-week-old rats (-5.6 ± 0.6 mV; $n = 6$) was not significantly different from that produced by similar ACh applications in neurons from younger animals (mean response in younger animals was -5.0 ± 0.6 mV; $n = 10$; $p = 0.5$), indicating that hyperpolarizing responses to transient mAChR activation also occur in adult animals.

Finally, because mAChRs require intracellular signal transduction via G-protein-linked cascades, it is possible that our use of whole-cell recording could modify normal cholinergic signaling. To confirm that mAChR-induced hyperpolarizations do not result from intracellular changes attributable to whole-cell recording, we made extracellular recordings from identified layer 5 pyramidal neurons while neurons were driven to fire action potentials spontaneously by increased extracellular potassium (6 mM) and bath application of the glutamate receptor agonist kainate (200 nM). Under these conditions, in six of six neurons, focal application of ACh (20 ms) to the soma produced a prolonged inhibition of action potential firing (Fig. 1*H*). For these experiments, the mean duration of inhibition was 1640 ± 270 ms, and the instantaneous spike frequency (ISF) was reduced from 13.8 ± 2.7 to 0.6 ± 0.1 Hz ($n = 6$; $p < 0.01$).

Pharmacology of mAChR-mediated hyperpolarization

Muscarinic receptors have been broadly classified into two distinct families based on their coupling to intracellular messengers. Members of the M_1-type family (M_1, M_3, and M_5) are generally associated with G_q signaling and phosphatidylinositol turnover. In contrast, members of the M_2-type family (M_2 and M_4) are generally linked via G_i to cAMP production. To determine the receptor family responsible for mediating ACh-induced hyperpolarizations, we focally applied ACh (1 s) before and after exposing slices to selective muscarinic antagonists. Bath application (5 min) of the M_1-type-selective antagonist pirenzepine (PZP) (500 nM) completely blocked ACh-induced hyperpolarizing responses ($n = 6$) (Fig. 2*A*,*C*). In control conditions, ACh applications for 1 s produced hyperpolarizing responses of -5.2 ± 1.0 mV and delayed depolarizations of 4.7 ± 0.8 mV ($n = 6$). After PZP application, hyperpolarizing responses were no longer observed, with the mean change in membrane potential at a time corresponding to the peak hyperpolarization in control conditions being $+1.6 \pm 0.7$ mV ($n = 6$; $p < 0.01$). Similarly, the delayed depolarizing phase was significantly reduced by PZP, being reduced to only $+1.2 \pm 0.4$ mV at a time corresponding to the peak depolarization in control conditions ($n = 6$; $p < 0.01$). Conversely, in a separate group of neurons, bath application of the M_2-selective antagonist methoctramine (MCT) (500 nM; 5 min) had no effect on hyperpolarizing responses to 1-s-long applications of ACh ($n = 6$) (Fig. 2*B*,*D*). In these neurons, the peak amplitude of hyperpolarizing and depolarizing responses in control were -4.1 ± 0.7 and 5.0 ± 1.3 mV, respectively. After the bath application of MCT, hyperpolarizing responses to ACh were of identical amplitude (-4.1 ± 0.5 mV), whereas peak depolarizing responses were slightly, but not significantly, larger, with the mean depolarization in MCT being 7.1 ± 1.8 mV ($n = 6$; $p = 0.7$) (Fig. 2*D*).

The data above indicate that both hyperpolarizing and depolarizing responses to brief (1 s) ACh applications require M_1-type receptor activation. Furthermore, the finding that atropine and PZP completely block hyperpolarizing ACh responses, whereas carbachol mimics the effect of ACh, strongly suggest that nicotinic receptors play little, if any, role in their generation. To compare the depolarization generated by brief ACh applications with the depolarization commonly observed during tonic mAChR activation, we bath applied carbachol (10 μM) to control slices and slices continuously exposed to either PZP (500 nM; $n = 6$) or MCT (500 nM; $n = 5$). In control neurons, bath application of carbachol (5 min) depolarized neurons by 4.9 ± 0.3 mV ($n = 15$;

Table 1. Comparison of hyperpolarizing responses to 1 s applications of carbachol or ACh

Agonist	*n*	Resting V_m (mV)	Latency (ms)	Rise time (ms)	Amplitude (mV)	Half-width (ms)
Carbachol	30	−79 ± 0.7	346 ± 29	238 ± 30	−4.8 ± 0.3	622 ± 89
Acetylcholine	21	−78 ± 0.9	342 ± 23	165 ± 11	−4.6 ± 0.5	489 ± 39

$p < 0.0001$), an amount similar to the peak amplitude of the depolarizing phase of responses to transient (1 s) mAChR activation with ACh (4.9 ± 0.7 mV; $n = 12$, data combined from baseline responses in the separate PZP and MCT experiments above). In neurons exposed to pirenzepine, bath application of carbachol (5 min) produced no significant depolarization (mean change in membrane potential was +0.3 ± 0.4 mV; $n = 6$; $p = 0.5$) (Fig. 2*C*), a result that was significantly different from the depolarization observed during 1-s-long applications of ACh in control conditions ($p < 0.001$). In contrast, in the presence of MCT, bath-applied carbachol (5 min) depolarized neurons by 6.2 ± 1.0 mV ($n = 5$; $p < 0.01$) (Fig. 2*D*), an amount not significantly different from the depolarization observed by transient (1 s) mAChR activation in control conditions ($n = 17$; $p = 0.3$). Together, these data suggest that the transient depolarization observed during focal ACh application is qualitatively and quantitatively similar to the depolarization observed during tonic carbachol application.

Previous studies demonstrating ACh-mediated hyperpolarization of neocortical pyramidal neurons during application of high concentrations of ACh (~10 mM) have suggested that the inhibitory actions of ACh are mediated by GABAergic synaptic transmission (McCormick and Prince, 1985, 1986). To test whether GABA mediates the ACh-induced hyperpolarizations described above, we focally applied ACh (1 s) in the continual presence of antagonists of $GABA_A$ and $GABA_B$ receptors. The presence of any of three $GABA_A$-specific antagonists, picrotoxin (100 μM; $n = 7$), bicuculline methiodide (20 μM; $n = 3$), or 2-(3-carboxypropyl)-3-amino-6-(4-methoxyphenyl)pyridazinium bromide (SR 95531) (10 μM; $n = 6$), delivered at concentrations sufficient to block GABAergic signaling, failed to block ACh-mediated hyperpolarizations (Fig. 3). Similarly, the presence of the $GABA_B$ receptor antagonist (2*S*)-3-[[(15)-1-(3,4-dichlorophenyl)ethyl]amino-2-hydroxypropyl](phenylmethyl)phosphinic acid (CGP 55845) (1 μM; $n = 6$) had no effect on ACh-mediated hyperpolarizing responses (Fig. 3). No significant differences were observed in the mean amplitudes of hyperpolarizing responses generated in control conditions (mean response, −4.6 ± 0.5 mV; $n = 21$) (Table 1) and responses generated in the presence of GABAergic antagonists (ANOVA; $p = 0.68$) (Fig. 3*B*). The mean peak responses in GABA antagonists were −3.4 ± 0.8 mV (picrotoxin), −3.9 ± 0.5 mV (bicuculline), −4.2 ± 0.6 mV (SR 95531), and −5.0 ± 0.8 mV (CGP 55845). Together, these data demonstrate that ACh-induced hyperpolarizations require activation of M_1-type muscarinic receptors but do not involve increases in GABAergic synaptic transmission.

Hyperpolarizing responses are facilitated by calcium entry through voltage-gated calcium channels

To explore the impact of neuronal firing on transient cholinergic signaling, we compared responses to transient mAChR activation generated at resting potentials and during trains of action potentials. When ACh was repeatedly applied (five applications of 20 ms duration at 8 s intervals) to neurons at resting potentials (−78 ± 1 mV; $n = 9$), initial responses were quite large, with subsequent responses showing rapid reduction in amplitude (Fig. 4*A*). Compared with the initial hyperpolarization, responses to applications 2 through 5 were reduced by 73 ± 9, 80 ± 6, 87 ± 6, and 86 ± 5%, respectively ($n = 9$; $p < 0.001$).

In the same neurons, ACh applications were repeated during periods of repetitive action potential firing generated by somatic current injection (Fig. 4*A*,*C*). Under these conditions, responses to the first application of ACh were significantly more hyperpolarizing than were initial responses generated at rest (−4.8 ± 0.6 mV compared with −3.4 ± 0.3 mV at rest; $n = 9$; $p < 0.05$). Furthermore, membrane depolarization prevented response rundown during repeated applications, with responses being reduced by only 2 ± 10, −3 ± 10, 3 ± 11, and 13 ± 12% for applications 2 through 5, respectively ($n = 9$; $p = 0.32$). Additional experiments revealed that brief periods of action potential firing (4 or 5 s), delivered immediately before a test application of ACh or carbachol, prevented response rundown to repeated ACh applications at the resting potential (data not shown; see also Fig. 7*C* below). This procedure was used throughout the experiments described in this manuscript to obtain reproducible responses to repeated ACh or carbachol applications.

To determine whether action potentials themselves are necessary to prevent response rundown, in a separate group of neurons, we blocked action potentials by including TTX (1 μM) in the aCSF while delivering repetitive focal applications of ACh (20 ms; five applications at 8 s intervals). In the presence of TTX, and with membrane potentials adjusted to −60 mV with current injection to mimic action potential threshold, responses to focal ACh applications 2 through 5 were reduced by 67 ± 8, 75 ± 6, 71 ± 6, and 82 ± 7%, respectively ($n = 11$; $p < 0.0001$), amounts that were similar to those observed at resting potentials without TTX present (Fig. 4*B*,*C*). Although these data suggest that TTX-sensitive action potentials are required to reduce rundown, when the same neurons were further depolarized by strong current injection (600–900 pA) to membrane potentials above −50 mV (mean, −42 ± 3 mV), responses 2 through 5 were reduced by only 9 ± 3, 6 ± 4, 7 ± 5, and 10 ± 5% ($n = 11$; $p < 0.05$) (Fig. 4*B*,*C*), indicating that depolarization in the absence of action potentials can prevent response rundown.

Another potential mechanism by which depolarization might facilitate mAChR-mediated responses is through the activation of voltage-gated calcium channels (VGCCs) and subsequent increases in intracellular calcium. To determine whether VGCCs play a role in promoting hyperpolarizing responses to mAChR activation, in a subset of neurons previously exposed to TTX ($n = 10$), we bath applied the broad-spectrum VGCC antagonist cadmium chloride (200 μM, 5 min exposure) while repeatedly applying ACh (five applications of 20 ms at 8 s intervals). In the presence of both TTX and cadmium, and with strong somatic depolarization to membrane potentials above −50 (mean membrane potential, −41 ± 2 mV), responses 2 through 5 were reduced by 52 ± 10, 46 ± 4, 57 ± 5, and 65 ± 4%, respectively ($n = 10$; $p < 0.0001$) (Fig. 4*B*,*C*). In five of these neurons, we washed out cadmium for 20 min and observed a partial reversal of the effects of cadmium. In these neurons, responses 2 through 5 were reduced by 15 ± 9, 11 ± 7, 24 ± 8, and 23 ± 10%, respectively ($n = 5$; $p = 0.1$).

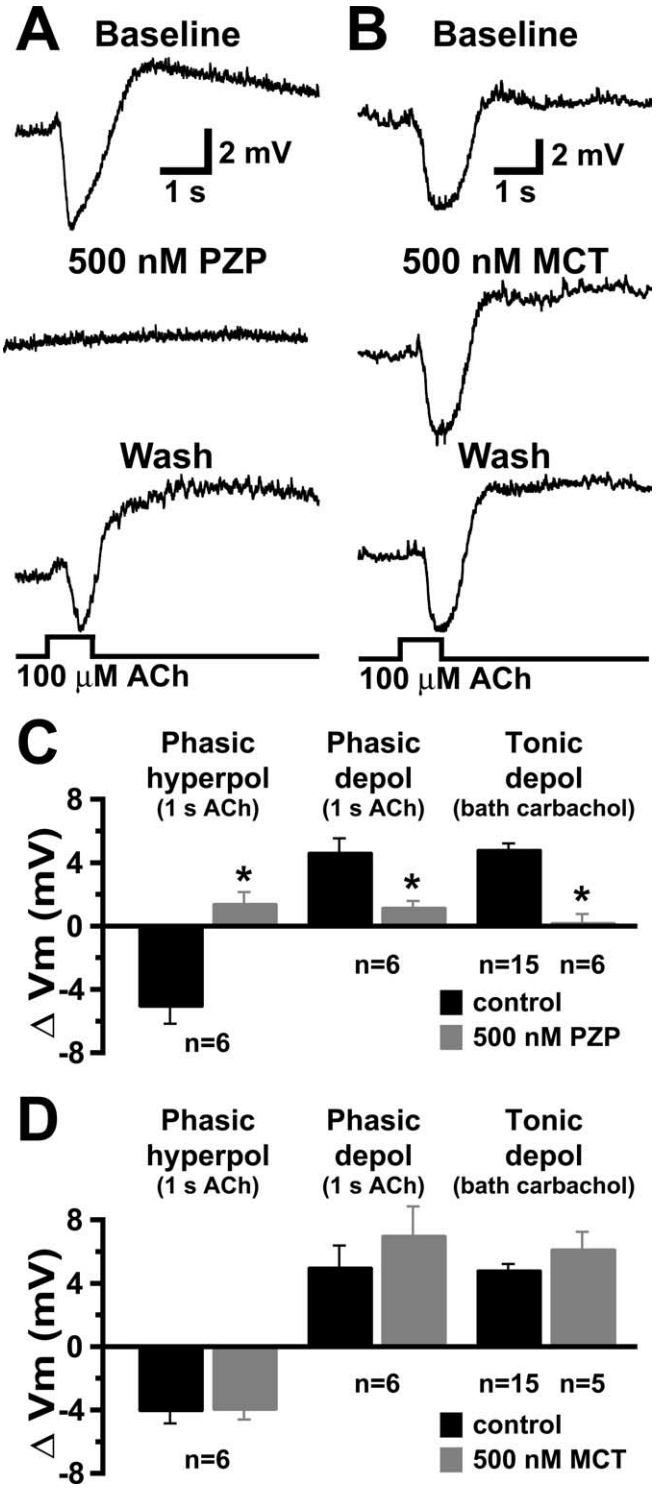

Figure 2. Cholinergic inhibition results from M_1 receptor activation. ***A***, Responses of a layer 5 neuron to transient ACh application (1 s) in control conditions (top trace) and after a 5 min bath application of the M_1 receptor antagonist PZP (500 nM; middle trace). The response partially returns after a 20 min wash in control aCSF (bottom trace). ***B***, Cholinergic responses before (top trace), during (middle trace), and after (bottom trace) a 5 min bath application of the M_2 receptor antagonist MCT (500 nM). ***C***, Summary graph showing the effects of PZP on hyperpolarizing and depolarizing responses to 1-s-long ACh applications ($n = 6$), as well as on tonic depolarization generated by a 5 min bath application of carbachol (10 μM; $n = 15$ in control condition; $n = 6$ in PZP). ***D***, Summary graph showing the effects of MCT on hyperpolarizing and depolarizing responses to 1-s-long ACh applications ($n = 6$), as well as on tonic depolarization generated by a 5 min bath application of carbachol (10 μM; $n = 5$ in MCT). Control cells for bath-applied carbachol data are the same for ***C*** and ***D***.

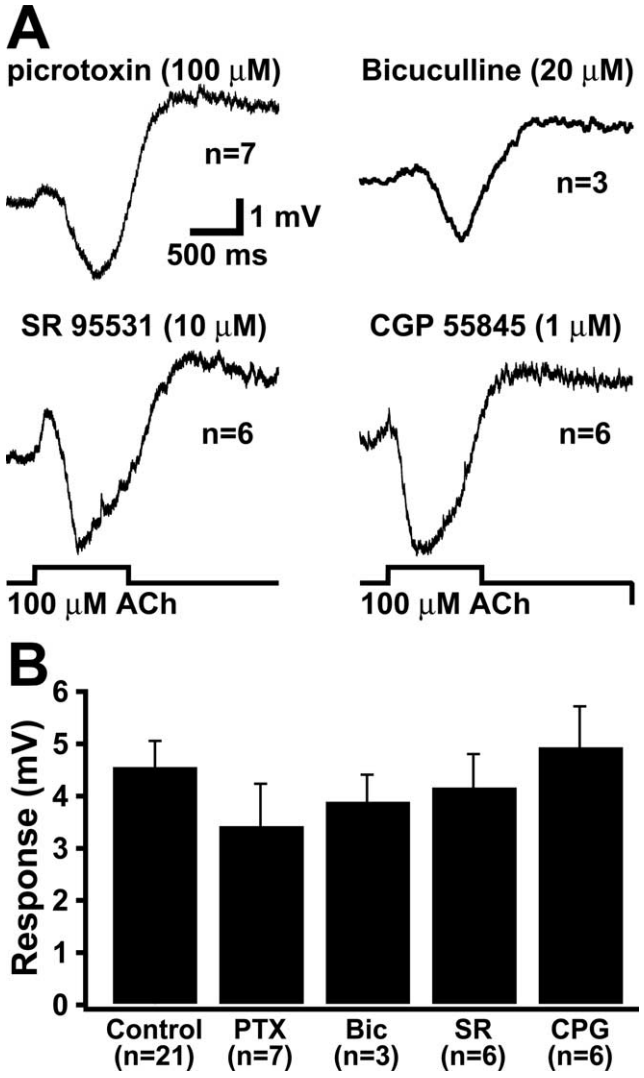

Figure 3. Transient cholinergic inhibition is not mediated by a GABAergic mechanism. ***A***, Responses of pyramidal neurons to focal application of ACh (100 μM; 1 s) in the presence of a variety of GABAergic antagonists: picrotoxin (PTX; top left), bicuculline (Bic; top right), SR 95531 (SR; bottom left), and CGP 55845 (CGP; bottom right). ***B***, A summary graph comparing the peak amplitudes of hyperpolarizing responses to ACh in control neurons ($n = 21$) with the peak amplitude of responses to ACh in the presence of the different GABAergic antagonists. All data from 1-s-long applications of ACh.

To examine the influence of VGCC on cholinergic hyperpolarizing responses in neurons at rest, in a separate group of neurons not exposed to TTX, we bath applied cadmium (200 μM; 5 min). In five neurons, baseline responses to ACh (40 ms) recorded in control conditions (mean amplitude, -3.4 ± 0.5 mV) were blocked after 5 min exposure to cadmium (Fig. 4*D*). In the presence of cadmium, the mean response amplitude was reduced to -0.4 ± 0.4 mV ($n = 5$; $p < 0.01$ when compared with baseline responses). Removal of cadmium from the bath partially rescued the cholinergic response in four of these neurons (mean response after wash, -1.7 ± 0.9 mV; $n = 5$). Together, the data above demonstrate that it is calcium entry through VGCCs, rather than action potentials per se, that is required to prevent the rundown of cholinergic hyperpolarizing responses.

Ionic mechanism of mAChR-mediated hyperpolarizations

The data above demonstrate that transient exposure to ACh produces a direct inhibitory effect on cortical pyramidal neurons that

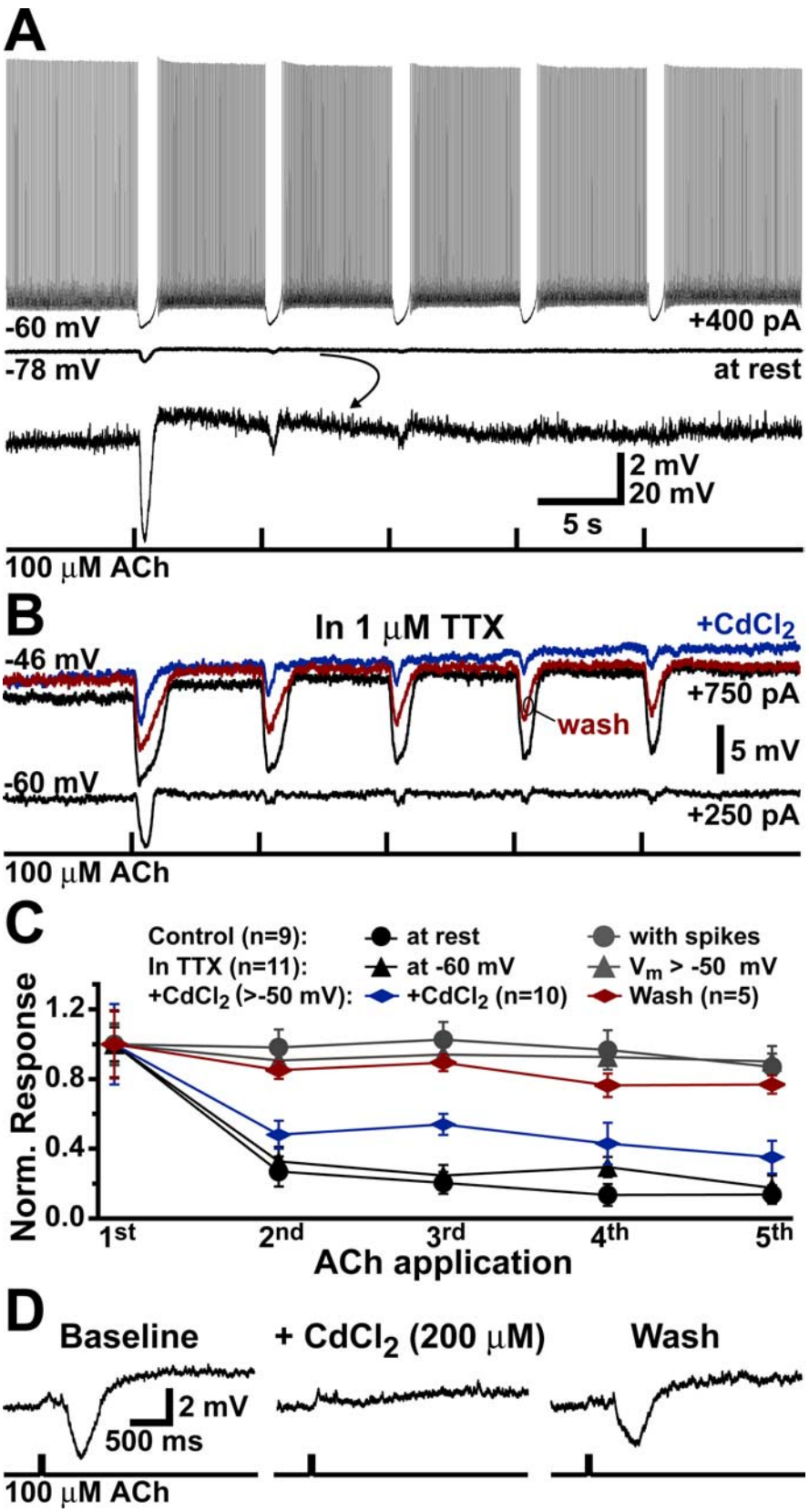

Figure 4. Calcium entry during trains of action potentials facilitates hyperpolarizing responses to transient mAChR activation. ***A***, Repeated application of ACh (20 ms applications at 8 s intervals) produces a gradual rundown of the hyperpolarizing response (bottom trace, expanded below for clarity). Repeating the protocol during a train of action potentials generated by a 400 pA current injection (top trace) facilitates phasic hyperpolarizing responses. ***B***, Responses to repetitive ACh application (20 ms at 8 s intervals) in a neuron exposed to 1 μM TTX at −60 mV (bottom black trace) and during strong depolarization (top black trace). Subsequent bath application of cadmium (200 μM) caused significant rundown at the depolarized potential (blue trace), an effect that was partially reversed after 20 min wash in regular aCSF (red trace). ***C***, Summary graph comparing the amplitude of hyperpolarizing responses for each of five ACh applications in control cells at rest and when depolarized (circles; $n = 9$), in a separate group of neurons exposed to 1 μM TTX at −60 mV and during strong depolarization (triangles; $n = 11$), and a subset of neurons transiently exposed to cadmium (diamonds; $n = 10$; $n = 5$ for wash). ***D***, Bath application of cadmium chloride (200 μM) in the absence of TTX reversibly eliminates the hyperpolarizing response to a 40 ms ACh application at resting potentials.

is not mediated by the synaptic release of GABA. Furthermore, the data above demonstrating that cadmium, but not TTX, antagonizes cholinergic signaling suggests that intracellular calcium may play a role in generating hyperpolarizing responses to ACh. To confirm that intracellular calcium is important for mAChR signaling, we filled patch pipettes with an internal solution including the calcium-chelating agent BAPTA (10 mM). In six of six neurons, the presence of BAPTA completely blocked hyperpolarizing responses to 1-s-long applications of ACh, with the mean change in membrane potential after ACh application being $+1.3 \pm 0.2$ mV within 5 min after obtaining a whole-cell recording (Fig. 5*B*). Because the presence of BAPTA in the recording pipette blocked responses immediately, it was impossible to compare responses before and after BAPTA application. As an added control, in four additional neurons, we made whole-cell recordings of hyperpolarizing responses with pipettes filled with regular intracellular solution (no BAPTA) before repatching with a BAPTA-containing pipette (Fig. 5*A*). In all four neurons, hyperpolarizing responses to ACh that were observed when pipettes were filled with regular intracellular solution (mean response was -4.2 ± 0.7 mV) were completely blocked when BAPTA was introduced during repatching (mean response at times matching peak hyperpolarization in first patches was $+0.6 \pm 0.3$ mV). In a separate group of four neurons, we repatched neurons with regular pipette saline without BAPTA. In this control group, hyperpolarizing responses to ACh after repatching were similar to the mAChR responses observed during the first patch recording (mean response to ACh after repatching was -3.6 ± 1.0 mV; $n = 4$; $p = 0.52$; data not shown). These data demonstrate a necessity for free intracellular calcium in the generation of hyperpolarizing responses to ACh.

We next determined the reversal potential for ACh responses by transiently

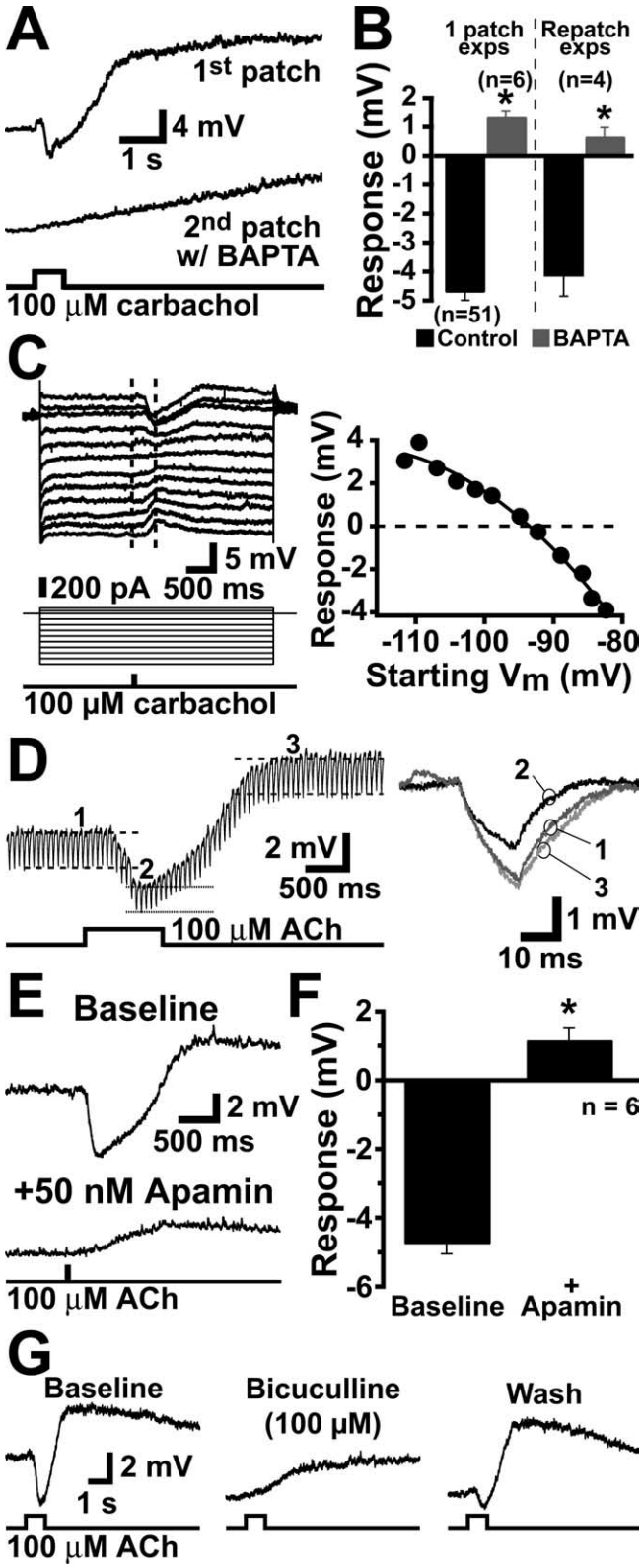

Figure 5. Hyperpolarizing responses to transient mAChR stimulation result from the activation of an SK-type calcium-activated potassium conductance. ***A***, Responses of a pyramidal neuron to transient carbachol application when patched with normal internal pipette solution (top trace) and after being patched a second time with a pipette containing the calcium-chelating agent BAPTA (10 mM; bottom trace). ***B***, Summary graph showing effectiveness of internal BAPTA in blocking cholinergic responses. The left two bars show a comparison of responses to 1-s-long applications of carbachol or ACh in control conditions ($n = 51$) and in cells patched a single time with BAPTA (10 μM) in the pipette ($n = 6$). Right two bars compare responses to carbachol (1 s) in control conditions and after repatching with a BAPTA-containing pipette (10 μM; $n = 4$). ***C***, Responses to a 40 ms application of carbachol (100 μM; top) from different starting potentials generated by somatic current injection (bottom). Right, A plot of peak response versus starting potential indicates a reversal potential of -94 mV. ***D***, ACh-induced hyperpolarizations are associated with an increased membrane conductance. The membrane response to repetitive current injections is shown during the focal application of ACh (1 s). Thick dashed lines indicate the amplitude of membrane responses to somatic current steps in baseline conditions (shown again during the depolarizing phase of the Ach response for comparison). Thin dotted lines show the amplitude of responses to current injection during the peak of the ACh-induced hyperpolarization. To the right are enlarged traces of individual hyperpolarizing pulses generated before (1), during (2), and after (3) application of ACh. ***E***, The application of the SK-type potassium channel blocker apamin irreversibly blocks the hyperpolarizing response to transient mAChR activation (40 ms). ***F***, Summary graph showing that apamin completely blocks ACh-induced hyperpolarizations. ***G***, Bath application of 100 μM bicuculline methiodide, an SK channel antagonist at high concentrations, reversibly blocks hyperpolarizing responses to ACh.

applying ACh to neurons while manipulating the membrane potential by somatic current injection (Fig. 5*C*). The mean reversal potential for ACh responses was -93 ± 1 mV ($n = 10$), a value close to the expected reversal potential for potassium (-98 mV), suggesting that mAChR-mediated hyperpolarizations result from activation of a potassium conductance. Indeed, mAChR activation was associated with a significant increase in membrane conductance (Fig. 5*D*). In a subset of neurons, hyperpolarizing pulses (-200 pA, 15 ms duration, at 15 Hz) were generated repeatedly while ACh ($n = 8$) or carbachol ($n = 4$) was focally applied to neurons, and the hyperpolarization generated from these negative current pulses was compared between different phases of the response (mean of three consecutive events immediately before drug application, at the peak of the hyperpolarizing response, and 1.5 s after the hyperpolarizing response were compared). In these neurons, mAChR activation produced an increase in membrane conductance of $31 \pm 5\%$ during the peak of the hyperpolarizing response ($n = 12$; $p < 0.05$). Conversely, at 1.5 s after the drug application, during the depolarizing phase of the response, whole-cell conductance was slightly, but significantly, decreased by $10 \pm 3\%$ ($p < 0.001$).

Because hyperpolarizing responses to ACh result from activation of a membrane conductance that reverses near the equilibrium potential for potassium, and, given their dependency on intracellular calcium, we tested the hypothesis that mAChR activation hyperpolarizes layer 5 pyramidal neurons by activating calcium-activated potassium channels. Bath application of apamin (50 or 100 nM; 5 min exposure), an antagonist of SK-type calcium-activated channels, completely and irreversibly blocked all hyperpolarizing responses to focal ACh application (40 ms) (Fig. 5*E*,*F*). In baseline conditions, ACh application generated hyperpolarizing responses of -4.8 ± 0.3 mV. After apamin application for 5 min, ACh-mediated hyperpolarizations were completely abolished, with the mean change in membrane potential being $+1.2 \pm 0.4$ mV at a time corresponding to the peak hyperpolarization in baseline conditions ($n = 6$; $p < 0.05$). Another substance known to block SK-type channels nonspecifically is the $GABA_A$ channel antagonist bicuculline methiodide (Johnson and Seutin, 1997). In contrast to the lack of effect seen with low concentrations (20 μM) of bicuculline, bath application of bicuculline at a higher concentration (100 μM) for 5 min reversibly blocked hyperpolarizing responses to mAChR activation (Fig. 5*G*). In baseline conditions, 1-s-long applications of ACh generated hyperpolarizations of -3.1 ± 0.4 mV. After a 5 min bath application of bicuculline, the mean change in membrane potential at the time of peak hyperpolarization in baseline conditions was 0.0 ± 0.2 mV ($n = 10$; $p < 0.001$). After 10–15 min of wash

in regular aCSF, responses returned to −2.6 ± 0.6 mV. Together, these data demonstrate that ACh hyperpolarizes neocortical pyramidal neurons through the activation of SK-type potassium channels.

mAChR-dependent intracellular calcium signaling

The data presented above indicate that mAChR activation in pyramidal neurons triggers an increase in intracellular calcium concentration. To observe this directly, we loaded neurons with the low-affinity calcium-sensitive dye OGB6F (100 μM) and focally applied ACh while measuring somatic fluorescence with confocal microscopy (Fig. 6) (supplemental videos 1, 2, available at www.jneurosci.org as supplemental material). Hyperpolarizing responses to focal ACh applications (5–20 ms) were associated with increases in intracellular calcium, as indicated by increases in fluorescence during line scans through the longitudinal axis of the soma (Fig. 6*A*). Consistent with the facilitatory action of neuronal depolarization described above (Fig. 4*A–C*), the amplitude of ACh-induced increases in fluorescence was 51 ± 20% larger when ACh was applied during periods of action potential firing ($n = 5$; $p < 0.01$) (Fig. 6*B*). When responses generated at resting potentials were analyzed (17 trials in 5 neurons), a statistically significant correlation was observed between peak Δ*F*/*F* and the amplitude of the corresponding hyperpolarizing voltage response ($n = 21$; $p < 0.01$) (Fig. 6*C*).

During the imaging experiments described above, short applications of ACh were used to limit the depolarizing phase of the ACh response. To compare calcium signaling during hyperpolarizing and depolarizing responses, we imaged calcium transients during 1-s-long ACh applications (Fig. 6*D*,*E*). To limit movement artifacts during 1-s-long ACh applications, pipettes were positioned ~30 μm from the soma, and pressure was reduced to ~5 psi. Under these conditions, ACh application produced biphasic, hyperpolarizing then depolarizing responses. The peak hyperpolarization in these responses was −2.8 ± 0.4 mV, whereas the peak depolarization was 5.3 ± 0.9 mV (Fig. 6*D*). To compare calcium signaling during the two phases, we measured Δ*F*/*F* at the peak of the hyperpolarizing and depolarizing responses (Fig. 6*D*,*E*). During the peak of the hyperpolarizing response, Δ*F*/*F* was 1.05 ± 0.09. Conversely, Δ*F*/*F* at the peak of depolarizing responses was significantly less ($n = 4$; $p < 0.001$), being very close to zero (mean Δ*F*/*F* at peak depolarization was 0.02 ± 0.01; $n = 4$). Our finding that internal calcium levels are not increased during the depolarizing phase of ACh responses is consistent with previous data showing that bath application of carbachol alone does not produce calcium signals in these neurons (Larkum et al., 2003).

Because the increases in intracellular calcium described above were coincident with hyperpolarization but not depolarization of the membrane potential, they are unlikely to be attributable to activation of VGCCs. Therefore, we hypothesized that mAChR activation induces the release of calcium from intracellular stores. To test for this, we emptied intracellular calcium stores with bath-applied cyclopiazonic acid (CPA) (30 μM). Five minutes of exposure to CPA completely blocked ACh-induced hyperpolarizing responses ($n = 6$) (Fig. 7*A*). In control conditions, brief applications of ACh (20 ms) produced a 4.1 ± 0.6 mV hyperpolarization of the membrane potential. After CPA application, all hyperpolarizing responses were absent, revealing a small depolarization of 0.9 ± 0.2 mV ($n = 6$; $p < 0.001$) (Fig. 7*B*).

Calcium release from intracellular stores can be mediated by two ligand-gated channels in the endoplasmic reticulum: ryanodine-sensitive receptors and IP_3-sensitive receptors. To test for a role of ryanodine receptors in mAChR signaling, we repeatedly applied ACh (40 ms duration, 15 s intervals) while bath applying ryanodine to interfere with ryanodine receptor signaling (Fig. 7*C*). Bath application of ryanodine (20 μM; 10 min) led

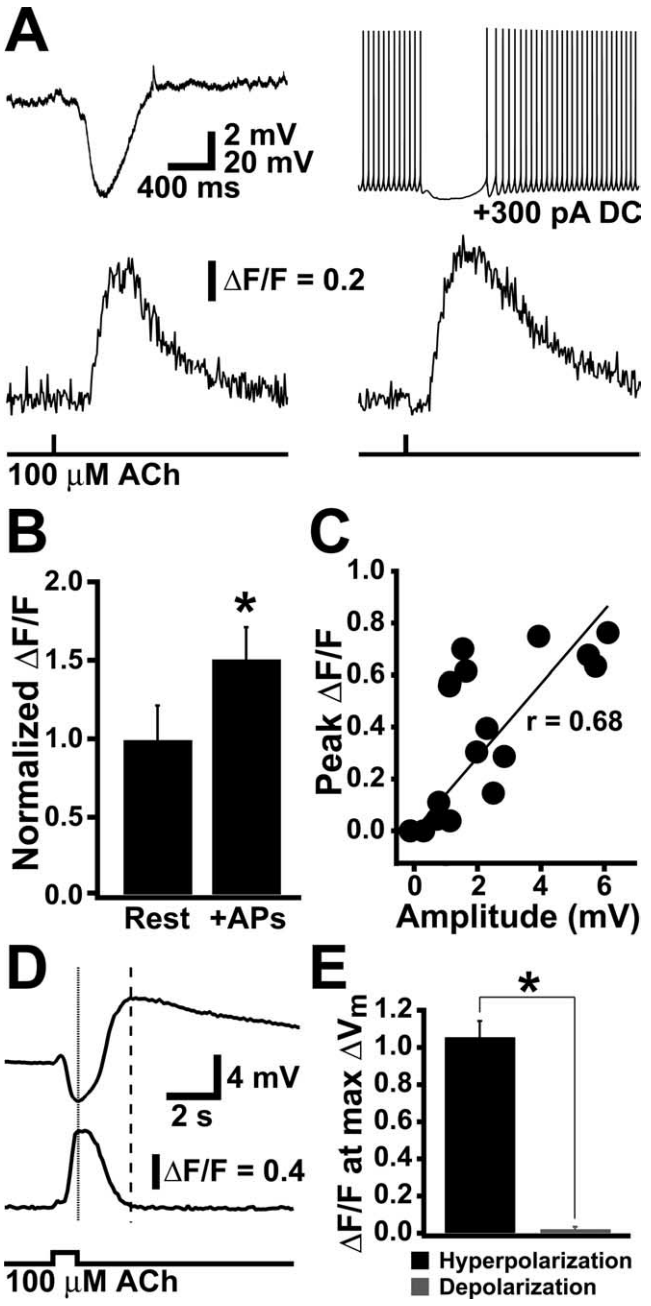

Figure 6. Calcium-imaging experiments demonstrate a rise in internal calcium that is correlated with the timing and magnitude of hyperpolarizing responses to ACh. ***A***, Voltage (top) and optical (Δ*F*/*F*; bottom) responses of a pyramidal neuron to a 5 ms application of ACh at rest (left) and during a train of action potentials generated by somatic current injection (right). DC, Direct current. ***B***, Summary data showing that the peak Δ*F*/*F* is larger when generated during action potential (AP) firing ($n = 5$). ***C***, Plot of the correlation between peak Δ*F*/*F* and the magnitude of the hyperpolarizing response from rest. Data are from multiple trials in five neurons experiencing ACh applications of 5–20 ms duration. ***D***, The membrane response (top) and Δ*F*/*F* measured from a line scan across the soma (bottom) during a 1-s-long application of ACh. Traces are the average of five consecutive ACh applications. The dotted line shows timing of peak hyperpolarization, and the dashed line demarks peak depolarization. ***E***, Summary graph comparing Δ*F*/*F* values at the peak of the depolarizing and hyperpolarizing phases of responses to 1-s-long applications of ACh ($n = 4$).

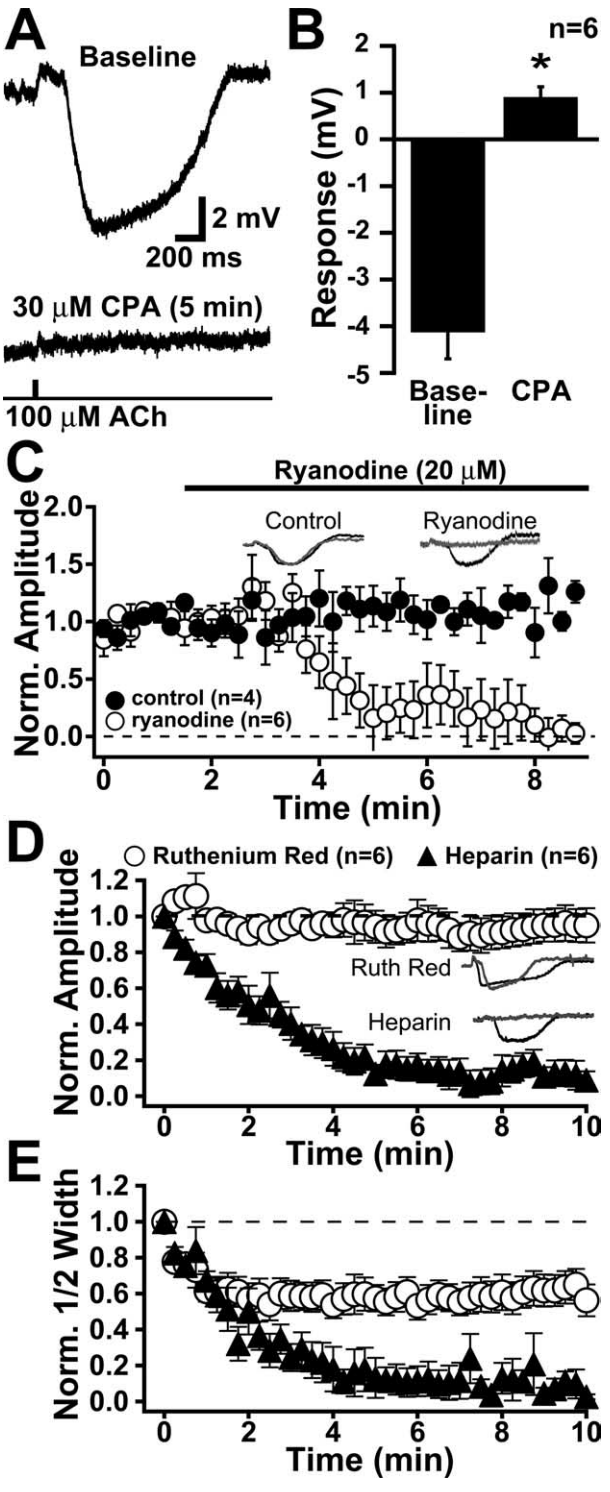

Figure 7. Transient mAChR activation leads to calcium release from IP_3-sensitive stores. ***A***, Response to a 20 ms application of ACh in control conditions (top) and after a 5 min bath application of CPA. ***B***, Summary data from six experiments in which CPA was applied. Hyperpolarizing responses were completely eliminated after 5 min exposure to CPA. ***C***, Plot of normalized peak hyperpolarizing response amplitude for ACh applications given at 15 s intervals in control conditions (filled circles) and after bath application of ryanodine (20 μM; open circles). Insets, Superimposed traces of from the beginning (black) and end (gray) of the experiment for control and ryanodine-exposed neurons. ***D***, ***E***, Patching neurons with pipettes filled with either the ryanodine receptor antagonist ruthenium red (open circles) or the IP_3 receptor antagonist heparin (filled triangles) demonstrates that the peak amplitude of hyperpolarizing responses depends solely on IP_3 receptor activation (***D***), whereas activation of ryanodine receptors can prolong response half-width (***E***). Insets, The first (black) and last (gray) traces superimposed for cells patched with heparin or ruthenium red.

to a rapid decreased in response amplitude by 95 ± 2% ($n = 6$; $p < 0.01$) (Fig. 7*C*).

Although the ability of ryanodine to block mAChR-mediated hyperpolarizations is suggestive of a role for ryanodine receptors in gating ACh-induced calcium release, ryanodine and IP_3 receptors may share a common intracellular calcium store (Power and Sah, 2005). If so, it is possible that activation of ryanodine receptors with bath-applied ryanodine may deplete IP_3-sensitive calcium stores. To test the potential role of calcium release from IP_3-sensitive stores, we patched neurons with pipettes filled with a solution containing the IP_3 receptor blocker heparin (2–3 mg/ml) and measured hyperpolarizing responses to applications of ACh presented at 15 s intervals beginning immediately after the attainment of whole-cell recording (Fig. 7*D*,*E*). The addition of intracellular heparin produced a steady decrease in the peak amplitude and half-width of ACh-induced hyperpolarizing responses to 6 ± 1 and 2 ± 1% of their original amplitude, respectively, 10 min after the start of whole-cell recording ($n = 6$; $p < 0.001$) (Fig. 7*D*,*E*).

To further test the role of ryanodine receptors, in separate experiments, we added the ryanodine receptor antagonist ruthenium red (40 μM) to our pipette saline. Whereas intracellular ruthenium red produced no significant effect on the peak amplitude of responses (mean hyperpolarization after 10 min was 95 ± 9% of the initial response; $n = 6$; $p = 0.2$) (Fig. 7*D*), ruthenium red lead to a significant reduction in the half-width of hyperpolarizing responses by an average of 35 ± 9% ($n = 6$; $p < 0.05$) (Fig. 7*E*). Together, these data suggest that calcium release after activation of IP_3 receptors is both necessary and sufficient to generate ACh hyperpolarizing responses, but activation of ryanodine receptors can prolong ACh-induced hyperpolarizations.

Interaction of tonic and transient mAChR signaling

The above data demonstrate that phasic mAChR activation hyperpolarizes and decreases the excitability of neocortical pyramidal neurons. Conversely, tonic mAChR stimulation with bath-applied agonists depolarizes cortical pyramidal neurons, leading to an increase in excitability and, in some cases, spontaneous action potential generation. To determine whether phasic and tonic mAChR signaling can coexist in individual pyramidal neurons, we focally applied ACh (100 μM, 20 ms) before, during, and after bath application of carbachol (5 μM; 5–10 min exposure). In five of six neurons that experienced subthreshold depolarization in carbachol, additional mAChR activation with focally applied ACh generated transient hyperpolarizing responses (Fig. 8*A*). In a second set of neurons ($n = 6$), bath-applied carbachol (5 μM) combined with periodic depolarizing current steps (1 s, ~300 pA, 0.1 Hz) produced enough depolarization to initiate spontaneous and sustained action potential generation, presumably by accelerating voltage-dependent depolarization by carbachol (McCormick and Prince, 1986; Haj-Dahmane and Andrade, 1996). Under these circumstances, focal application of ACh continued to generate hyperpolarizing responses to inhibit action potential firing in 50% of neurons tested ($n = 3$ of 6 neurons firing spontaneously in carbachol) (Fig. 8*B*). Together, these data demonstrate that transient increases in mAChR activation can inhibit layer 5 neurons even during periods of tonic mAChR activation that is sufficient to depolarize neurons to action potential threshold.

One situation that may lead to increases in ambient concentrations of cortical ACh is the use of acetylcholinesterase inhibitors (AChEIs). These drugs, which are commonly prescribed to combat the cognitive deficits associated with Alzheimer's disease,

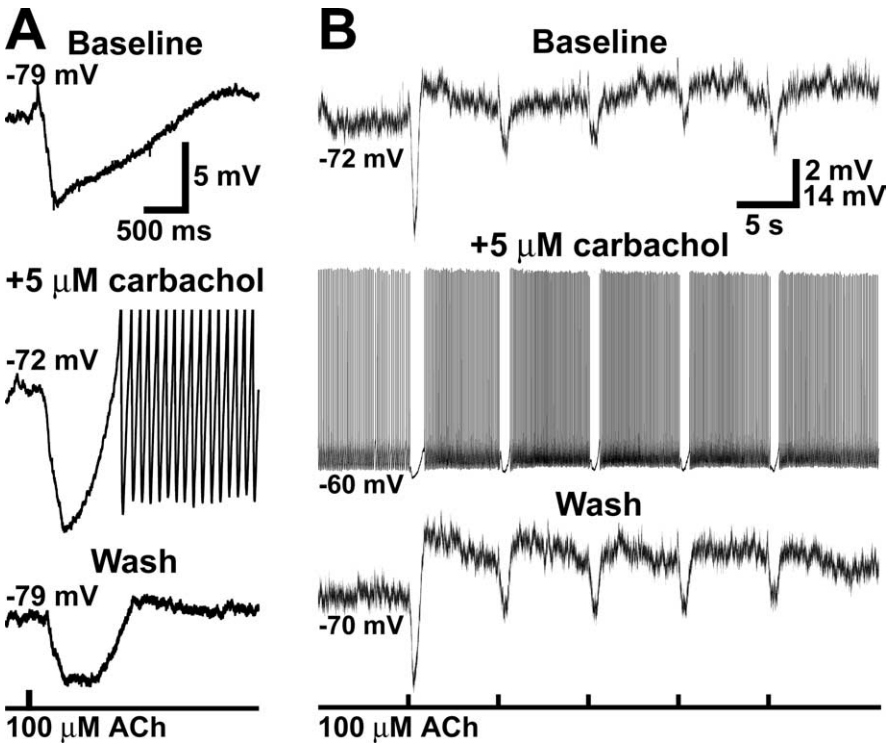

Figure 8. Coexistence of phasic inhibition with excitation from tonic mAChR activation. ***A***, Hyperpolarizing responses to focal ACh applications (20 ms) before (top trace), during (middle trace), and after (bottom trace) wash of 5 μM bath-applied carbachol. ***B***, A train of five applications of ACh (20 ms duration, 0.125 Hz) produces hyperpolarizing responses in baseline conditions (top trace). Although bath application of carbachol (5 μM) paired with several conditioning depolarizing pulses depolarized the neuron and induced spontaneous action potential generation, transient ACh application continued to produce hyperpolarizing responses during tonic firing (middle trace). The effect of ACh is still present after the removal of carbachol from the bath (bottom trace).

prevent the enzymatic breakdown of ACh in the brain. To investigate the impact of AChEIs, we focally applied ACh (1 s) to pyramidal neurons before and after bath application of eserine (Fig. 9*A*). Eserine (2 μM), an AChEI, moderately increased the mean amplitude of hyperpolarizing responses from -5.4 ± 0.4 to -6.5 ± 0.6 mV ($n = 17$; $p < 0.01$) and prolonged their half-width from 471 ± 46 to 598 ± 48 ms ($n = 17$; $p < 0.05$). More significantly, eserine dramatically enhanced depolarizing responses to ACh. In control conditions, 1-s-long ACh applications never induced spontaneous action potential generation on their own. When eserine was present, however, transient applications of ACh (1 s) produced sufficient depolarization to initiate action potential firing in 8 of the 17 neurons tested (47%; mean depolarization to threshold was 18 ± 1 mV). In the remaining neurons, in which the depolarizing phase of the mAChR response remained subthreshold, eserine significantly increased the amplitude of the depolarizing responses from 3.6 ± 0.4 to 5.8 ± 0.8 mV ($n = 9$; $p < 0.05$).

In contrast to the slight increase in the amplitude of inhibitory responses produced by eserine during single ACh applications, eserine reduced inhibition generated during repeated ACh applications (Fig. 9*B*,*C*). ACh was repeatedly applied to neurons during periods of suprathreshold somatic current injection (five applications at 8 s intervals) before and after the bath application of eserine (2 μM). In control conditions, the initial application of ACh reduced the ISF to 0.8 ± 0.09 Hz ($n = 9$; mean baseline ISF was 8 ± 1 Hz). The minimum ISFs generated by the subsequent four ACh applications were 1.2 ± 0.07, 1.1 ± 0.07, 1.1 ± 0.08, and 1.1 ± 0.07 Hz, respectively. When eserine was present, the baseline ISF generated by current injection increased to 13 ± 1 Hz ($p < 0.001$). Under these conditions, the initial application of ACh reduced the ISF to 0.7 ± 0.05 Hz ($n = 9$), a frequency similar to that observed in control conditions. Subsequent ACh applications, however, produced significantly less inhibition of action potential firing than in control conditions (Fig. 9*B*,*C*). In eserine, the minimum ISFs attained for applications 2 through 5 were 2.8 ± 0.6, 3.6 ± 0.8, 4.4 ± 1.1, and 5.0 ± 1.2 Hz, respectively ($n = 9$; $p < 0.05$). The rundown of individual hyperpolarizing responses during action potential firing in eserine was similar to the rundown observed in control neurons at rest ($p = 0.6$) (Fig. 4*C*), with responses 2 through 5 being reduced by 55 ± 12, 91 ± 28, 105 ± 30, and 109 ± 35%, respectively, when compared with the initial response ($n = 9$; $p < 0.0001$). Additional experiments showed that the increase in rundown of ACh-induced inhibition in the presence of eserine was not attributable to an eserine-induced increase in the ISF, because control cells with similar ISFs to those observed in eserine showed no obvious rundown (Fig. 9*D*,*E*). Together, these data demonstrate that AChEIs primarily enhance depolarization during single ACh applications but can decrease the inhibitory action of ACh when mAChRs are repeatedly activated during periods of intense somatic depolarization.

Discussion

The present study demonstrates, for the first time, that transient mAChR activation produces strong and direct inhibition of neocortical pyramidal neurons. Our data show that ACh, acting at M_1-type mAChRs, induces calcium release from IP_3-sensitive intracellular stores and subsequent activation of an apamin-sensitive, calcium-activated potassium conductance in neocortical pyramidal neurons (supplemental Fig. 1, available at www.jneurosci.org as supplemental material). This inhibition can be initiated by brief ($\geq$5 ms) ACh applications, can last for several seconds, and is strong enough to inhibit action potential generation even during periods of intense somatic depolarization. Remarkably, inhibitory responses to brief ACh applications were observed even during tonic mAChR activation that is sufficient to depolarize and drive action potential generation. Finally, we show that AChEIs enhance depolarization after transient mAChR activation but impede inhibition generated by repeated ACh applications. Together, these data demonstrate that ACh can directly inhibit cortical pyramidal neurons, and that this inhibition is less effective in the presence of AChEIs.

The direct SK-channel-dependent inhibitory action of transient mAChR activation in neocortical pyramidal neurons described here is similar to the inhibition generated in midbrain dopaminergic neurons after muscarinic (Fiorillo and Williams, 2000) or metabotropic glutamate (Fiorillo and Williams, 1998) receptor activation. Additionally, it is consistent with previous

work showing that increases in intracellular IP_3 lead to the activation of calcium-activated potassium conductances, including an SK-type conductance, in pyramidal neurons in mouse prefrontal cortex (Stutzmann et al., 2003) and rat visual cortex (Yamada et al., 2004). These previous data, together with our data from pyramidal neurons in rat somatosensory cortex, suggest that SK channel activation in response to the activation of G-protein-coupled receptors may be a generalized mechanism for inhibition in pyramidal neurons throughout the cortex. This cholinergic activation of apamin-sensitive SK channels contrasts with the well described block of the apamin-insensitive calcium-activated potassium channels underlying the slow afterhyperpolarization during tonic mACh activation in pyramidal neurons (Sah and Faber, 2002) and indicates that tonic and phasic mACh activation in the cortex are likely to have different functional roles.

Pharmacology of cholinergic signaling

Muscarinic transmission in the neocortex is critical for learning and memory (Winkler et al., 1995), and muscarinic antagonists impair memory in animals and people (Drachman and Leavitt, 1974; Buresova et al., 1986). The data presented here clearly support a role for muscarinic signaling in cortical processing. Our experiments using selective antagonists demonstrate that both the hyperpolarizing and depolarizing responses to ACh are mediated by M_1-type mAChRs. Of the M_1-familiy receptor subtypes (M_1, M_3, and M_5), M_1 receptors are by far the most abundant in the cerebral cortex, comprising up to 60% of all mAChRs expressed (Flynn et al., 1995). Because M_3 and M_5 receptors are expressed at very low levels in the cortex, it is likely that the direct actions of ACh on cortical pyramidal neurons are achieved primarily through M_1 receptor activation. M_1 receptors are classically linked via G_q and phospholipase C activation to the generation of two important signaling molecules: IP_3 (the endogenous ligand for IP_3 receptors) and diacylglycerol (DAG). DAG is an activator of protein kinase C, which can downregulate the M current (Schmitt and Meves, 1993). DAG can also directly activate some nonspecific cation conductances (Hofmann et al., 1999). If DAG does participate in the generation of depolarizing responses to ACh, the intrinsic bifurcation of the G_q signaling cascade would explain how both hyperpolarizing and depolarizing responses result from activation of the same receptor subtype. Tonic M_1 receptor stimulation by low, nonsaturating concentrations of bath-applied carbachol may favor depolarization via generation of only a modest increase in cytosolic IP_3 that is insufficient to evoke the large calcium increases required to activate SK channels. In contrast, additional M_1 receptor activation during focal applications of higher concentrations of ACh may increase intracellular IP_3 to a level sufficient to initiate substantial calcium release from intracellular stores and subsequent SK channel activation.

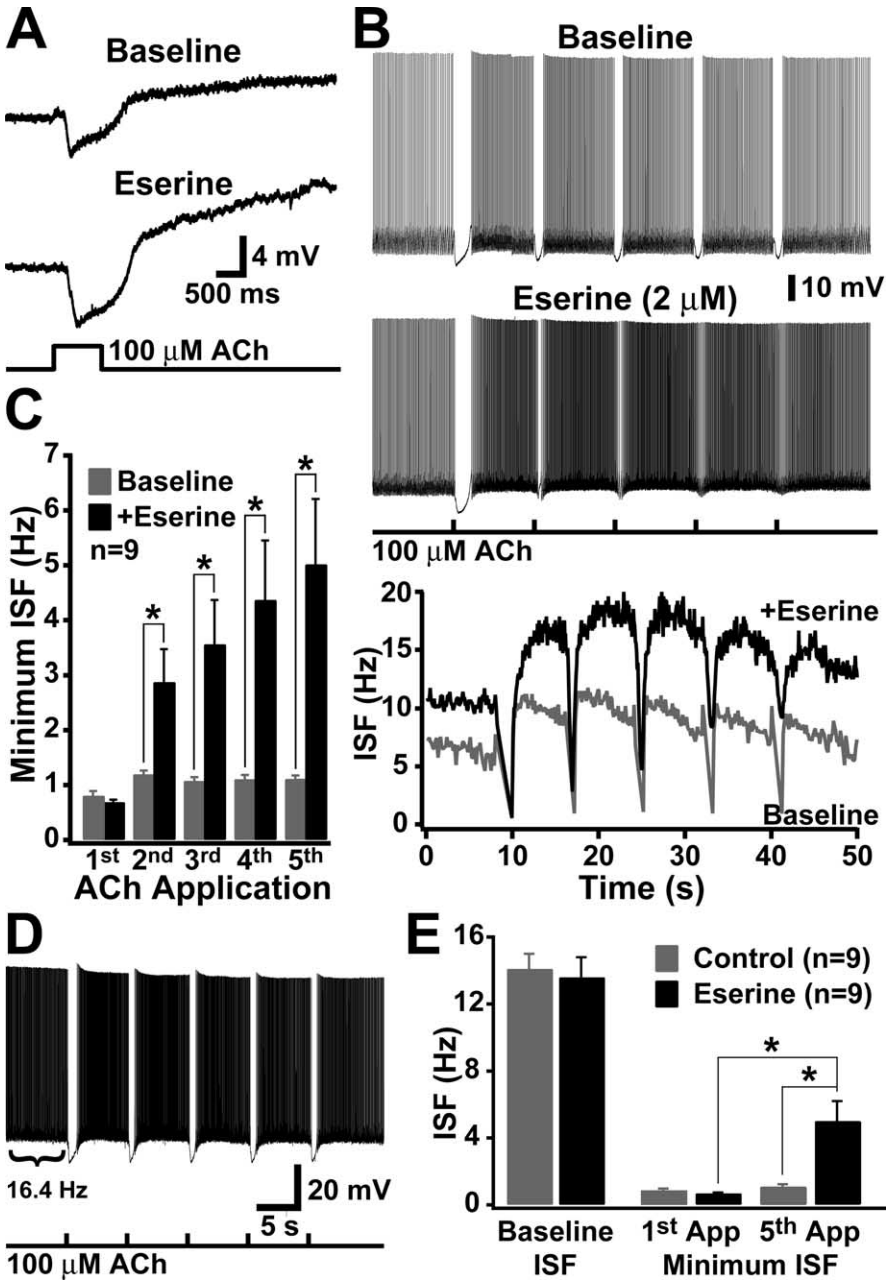

Figure 9. Impact of an acetylcholinesterase inhibitor on mAChR responses. ***A***, Responses to single applications of ACh (1 s) in control conditions (top trace) and after bath application of eserine (2 μM; bottom trace). ***B***, Responses to repeated ACh applications (20 ms, 8 s intervals) during action potential firing (+350 pA somatic current injection) before (top trace) and during (bottom trace) bath application of eserine. Bottom, Plots of the ISF showing the reduction in ISF for each of the five ACh applications in baseline conditions (gray trace) and in eserine (black trace). ***C***, Summary graph showing the mean minimum ISF attained during each of five ACh applications before (gray) and in eserine (black; $n = 9$). ***D***, Responses to ACh applications (20 ms) to a cell firing action potentials with a high ISF (mean ISF, 16.4 Hz) attained by somatic current injection (450 pA). ***E***, Summary graph comparing initial ISFs, as well as minimum ISFs attained during the first and fifth ACh application, in control neurons ($n = 9$) and neurons exposed to eserine (2 μM; $n = 9$; eserine data from neurons shown in ***B*** and ***C***). Significant changes in the minimum ISF were observed only in eserine-treated neurons.

Cholinergic inhibition in the cortex

Early experiments using intracellular recordings of neocortical pyramidal neurons showed that brief applications of very high concentrations of ACh (10 mM) often resulted in biphasic, hyperpolarizing then depolarizing, responses similar to those described here. McCormick and Prince (1986) attributed these mAChR-mediated hyperpolarizing responses to ACh-induced increases in GABA release. This conclusion was based on the finding that the reversal potential of the hyperpolarizing phase of ACh-mediated responses was similar to the reversal potential for GABA, and that traditional blockers of evoked GABAergic synaptic transmission (low extracellular Ca^{2+} or the presence of TTX, bicuculline, or picrotoxin) selectively blocked the hyperpolarizing phase of the response. Similar lines of reasoning were used to conclude that GABAergic mechanisms were responsible for hyperpolarizing responses observed during synaptic release of ACh in auditory cortex (Bandrowski et al., 2001), although in these experiments, synaptic responses were only partially sensitive to atropine and, therefore, likely involved activation of non-muscarinic receptors as well.

The data presented here indicate an additional mechanism whereby cholinergic inputs to pyramidal neurons will have a direct inhibitory effect on cortical pyramidal neurons independent of activation of local inhibitory networks. Given that high concentrations of bicuculline block cholinergic inhibition independently of $GABA_A$ receptor blockade (Fig. 5*F*), it seems likely that at least some the inhibitory actions of ACh described previously and attributed to GABA were actually mediated via the SK channel-dependent mechanism described here. For example, the studies by both McCormick and Prince (1986) and Müller and Singer (1989) used concentrations of bicuculline (50 μM or 1 mM) that would be expected to inhibit direct hyperpolarizing responses mediated by SK-type potassium channels (Fig. 5*F*). Furthermore, methods used to block synaptic transmission in previous studies, such as decreased extracellular calcium or the presence of TTX or cadmium, would be likely to prevent or slow the refilling of the calcium stores necessary for SK channel-mediated inhibition. Indeed, we found that the presence of either TTX (Fig. 4*B*,*C*) or cadmium (Fig. 4*D*) inhibited repetitive generation of hyperpolarizing responses at membrane potentials near rest. Furthermore, in several experiments, we found that storing slices in calcium-free saline eliminated hyperpolarizing responses to ACh (data not shown). In contrast, previous data describing picrotoxin-sensitive cholinergic hyperpolarization (McCormick and Prince, 1986; Bandrowski et al., 2001) may reflect differences in species (rats vs guinea pigs) or cortical region studied (somatosensory vs cingulate and auditory cortex). Additional studies, comparing the action of ACh in different cortical cell types and regions and *in vivo*, will be necessary to determine the relative impact of direct (SK-mediated) and indirect (GABA-mediated) cholinergic inhibition on cortical function.

Functional significance

Although muscarinic signaling in the cortex is critical for learning and memory, the way in which ACh facilitates these cognitive processes remains a mystery. One popular hypothesis suggests that ACh increases the signal-to-noise ratio of sensory input by tonically activating mAChRs to enhance the intrinsic neuronal excitability of cortical neurons while selectively reducing the size of corticocortical, rather than thalamocortical, excitatory inputs to neocortical pyramidal neurons (Hasselmo and Bower, 1992; Hasselmo and Cekic, 1996; Gil et al., 1997; Hsieh et al., 2000). This model assumes that ACh release in the cortex occurs via nonspecific volume transmission (Hasselmo and McGaughy, 2004). However, recent data point to a more cell-to-cell-specific coupling between cholinergic neurons and cortical targets, with cholinergic axon terminals associated with specialized postsynaptic densities, often occurring on the basal dendrites of pyramidal neurons (Mrzljak et al., 1995; Smiley et al., 1997; Turrini et al., 2001; Casu et al., 2002). Such specific connectivity implies that cholinergic release should lead to rapid and transient activation of postsynaptic mAChRs in cortical neurons and argues against a role of tonic mAChR activation via volume transmission. Consistent with this idea, in the absence of inhibitors of acetylcholinesterase, the ambient extracellular concentration of ACh in the brain is in the low nanomolar range (~20 nM) (Vinson and Justice, 1997) and is increased only twofold or threefold during behavioral states that promote ACh release in the cortex (Pepeu and Giovannini, 2004). Although the local concentration of ACh at synaptic mAChRs is not known, these findings suggest that the biphasic inhibitory/excitatory response to transient mAChR activation described here is likely to be more physiologically relevant than the tonic excitatory response observed during bath applications of micromolar concentrations of cholinergic agonists *in vitro*.

It is likely that both hyperpolarizing and depolarizing responses to transient mAChR activation influence information processing in the cortex. Hyperpolarizing responses to ACh may act to reset activity in layer 5 pyramidal neurons, whereas delayed cholinergic depolarization could enhance responsiveness to subsequent excitatory input and assist the refilling internal calcium stores to prevent rundown of hyperpolarizing responses over time. Furthermore, biphasic cholinergic signaling enhances the dynamic range of action potential firing frequencies during periods of sustained activation (Fig. 9*B*), which will influence information processing in the cortex.

Finally, the data presented here raise important questions about our current methods for treating ACh-related cognitive disorders such as Alzheimer's disease. The data from our eserine experiments suggest that AChEIs are likely to enhance the depolarizing action of ACh, while reducing the ability of ACh to inhibit neocortical pyramidal neurons. A complete understanding of how AChEIs interact with phasic and tonic mAChR signaling will require additional studies, the data from which may help explain why AChEIs have only modest efficacies in treating a disease in which ACh depletion is directly correlated with cognitive decline (Courtney et al., 2004).

References

Andrade R (1991) Cell excitation enhances muscarinic cholinergic responses in rat association cortex. Brain Res 548:81–93.

Bandrowski AE, Moore SL, Ashe JH (2001) Cholinergic synaptic potentials in the supragranular layers of auditory cortex. Synapse 41:118–130.

Bartus RT, Dean III RL, Beer B, Lippa AS (1982) The cholinergic hypothesis of geriatric memory dysfunction. Science 217:408–414.

Blitzer RD, Gil O, Landau EM (1990) Cholinergic stimulation enhances long-term potentiation in the CA1 region of rat hippocampus. Neurosci Lett 119:207–210.

Buresova O, Bolhuis JJ, Bures J (1986) Differential effects of cholinergic blockade on performance of rats in the water tank navigation task and in a radial water maze. Behav Neurosci 100:476–482.

Burgard EC, Sarvey JM (1990) Muscarinic receptor activation facilitates the induction of long-term potentiation (LTP) in the rat dentate gyrus. Neurosci Lett 116:34–39.

Casu MA, Wong TP, De Koninck Y, Ribeiro-da-Silva A, Cuello AC (2002) Aging causes a preferential loss of cholinergic innervation of characterized neocortical pyramidal neurons. Cereb Cortex 12:329–337.

Courtney C, Farrell D, Gray R, Hills R, Lynch L, Sellwood E, Edwards S, Hardyman W, Raftery J, Crome P, Lendon C, Shaw H, Bentham P (2004)

Long-term donepezil treatment in 565 patients with Alzheimer's disease (AD2000): randomised double-blind trial. Lancet 363:2105–2115.

Drachman DA, Leavitt JK (1974) Human memory and the cholinergic system. A relationship to aging? Arch Neurol 30:113–121.

Egorov AV, Hamam BN, Fransen E, Hasselmo ME, Alonso AA (2002) Graded persistent activity in entorhinal cortex neurons. Nature 420:173–178.

Egorov AV, Angelova PR, Heinemann U, Müller W (2003) Ca^{2+}-independent muscarinic excitation of rat medial entorhinal cortex layer V neurons. Eur J Neurosci 18:3343–3351.

Fiorillo CD, Williams JT (1998) Glutamate mediates an inhibitory postsynaptic potential in dopamine neurons. Nature 394:78–82.

Fiorillo CD, Williams JT (2000) Cholinergic inhibition of ventral midbrain dopamine neurons. J Neurosci 20:7855–7860.

Flynn DD, Ferrari-DiLeo G, Mash DC, Levey AI (1995) Differential regulation of molecular subtypes of muscarinic receptors in Alzheimer's disease. J Neurochem 64:1888–1891.

Gil Z, Connors BW, Amitai Y (1997) Differential regulation of neocortical synapses by neuromodulators and activity. Neuron 19:679–686.

Gloveli T, Egorov AV, Schmitz D, Heinemann U, Müller W (1999) Carbachol-induced changes in excitability and $[Ca^{2+}]_i$ signalling in projection cells of medial entorhinal cortex layers II and III. Eur J Neurosci 11:3626–3636.

Hagan JJ, Morris RGM (1988) The cholinergic hypothesis of memory: a review of animal experiments. In: Handbook of psychopharmacology (Iversen LL, Iversen SD, Snyder SH, eds), pp 237–323. New York: Plenum.

Haj-Dahmane S, Andrade R (1996) Muscarinic activation of a voltage-dependent cation nonselective current in rat association cortex. J Neurosci 16:3848–3861.

Haj-Dahmane S, Andrade R (1998) Ionic mechanism of the slow afterdepolarization induced by muscarinic receptor activation in rat prefrontal cortex. J Neurophysiol 80:1197–1210.

Halliwell JV (1989) Cholinergic responses in human neocortical neurones. EXS 57:138–149.

Hasselmo ME, Barkai E (1995) Cholinergic modulation of activity-dependent synaptic plasticity in the piriform cortex and associative memory function in a network biophysical simulation. J Neurosci 15:6592–6604.

Hasselmo ME, Bower JM (1992) Cholinergic suppression specific to intrinsic not afferent fiber synapses in rat piriform (olfactory) cortex. J Neurophysiol 67:1222–1229.

Hasselmo ME, Cekic M (1996) Suppression of synaptic transmission may allow combination of associative feedback and self-organizing feedforward connections in the neocortex. Behav Brain Res 79:153–161.

Hasselmo ME, McGaughy J (2004) High acetylcholine levels set circuit dynamics for attention and encoding and low acetylcholine levels set dynamics for consolidation. Prog Brain Res 145:207–231.

Hofmann T, Obukhov AG, Schaefer M, Harteneck C, Gudermann T, Schultz G (1999) Direct activation of human TRPC6 and TRPC3 channels by diacylglycerol. Nature 397:259–263.

Hsieh CY, Cruikshank SJ, Metherate R (2000) Differential modulation of auditory thalamocortical and intracortical synaptic transmission by cholinergic agonist. Brain Res 880:51–64.

Johnson SW, Seutin V (1997) Bicuculline methiodide potentiates NMDA-dependent burst firing in rat dopamine neurons by blocking apamin-sensitive Ca^{2+}-activated K^+ currents. Neurosci Lett 231:13–16.

Kasa P, Rakonczay Z, Gulya K (1997) The cholinergic system in Alzheimer's disease. Prog Neurobiol 52:511–535.

Klink R, Alonso A (1997) Muscarinic modulation of the oscillatory and repetitive firing properties of entorhinal cortex layer II neurons. J Neurophysiol 77:1813–1828.

Krnjevic K, Pumain R, Renaud L (1971) The mechanism of excitation by acetylcholine in the cerebral cortex. J Physiol (Lond) 215:247–268.

Larkum ME, Watanabe S, Nakamura T, Lasser-Ross N, Ross WN (2003) Synaptically activated Ca^{2+} waves in layer 2/3 and layer 5 rat neocortical pyramidal neurons. J Physiol (Lond) 549:471–488.

McCormick DA (1990) Cellular mechanisms of cholinergic control of neocortical and thalamic neuronal excitability. In: Brain cholinergic systems (Steriade M, Biesold D, eds), pp 236–264. Oxford: Oxford UP.

McCormick DA, Prince DA (1985) Two types of muscarinic response to acetylcholine in mammalian cortical neurons. Proc Natl Acad Sci USA 82:6344–6348.

McCormick DA, Prince DA (1986) Mechanisms of action of acetylcholine in the guinea-pig cerebral cortex in vitro. J Physiol (Lond) 375:169–194.

McCormick DA, Williamson A (1989) Convergence and divergence of neurotransmitter action in human cerebral cortex. Proc Natl Acad Sci USA 86:8098–8102.

Metherate R, Cox CL, Ashe JH (1992) Cellular bases of neocortical activation: modulation of neural oscillations by the nucleus basalis and endogenous acetylcholine. J Neurosci 12:4701–4711.

Mrzljak L, Pappy M, Leranth C, Goldman-Rakic PS (1995) Cholinergic synaptic circuitry in the macaque prefrontal cortex. J Comp Neurol 357:603–617.

Müller CM, Singer W (1989) Acetylcholine-induced inhibition in the cat visual cortex is mediated by a GABAergic mechanism. Brain Res 487:335–342.

Nishikawa M, Munakata M, Akaike N (1994) Muscarinic acetylcholine response in pyramidal neurones of rat cerebral cortex. Br J Pharmacol 112:1160–1166.

Ovsepian SV, Anwyl R, Rowan MJ (2004) Endogenous acetylcholine lowers the threshold for long-term potentiation induction in the CA1 area through muscarinic receptor activation: *in vivo* study. Eur J Neurosci 20:1267–1275.

Pepeu G, Giovannini MG (2004) Changes in acetylcholine extracellular levels during cognitive processes. Learn Mem 11:21–27.

Power JM, Sah P (2005) Intracellular calcium store filling by an L-type calcium current in the basolateral amygdala at subthreshold membrane potentials. J Physiol (Lond) 562:439–453.

Sah P, Faber ES (2002) Channels underlying neuronal calcium-activated potassium currents. Prog Neurobiol 66:345–353.

Schmitt H, Meves H (1993) Protein kinase C as mediator of arachidonic acid-induced decrease of neuronal M current. Pflügers Arch 425:134–139.

Schwindt PC, Spain WJ, Foehring RC, Chubb MC, Crill WE (1988) Slow conductances in neurons from cat sensorimotor cortex *in vitro* and their role in slow excitability changes. J Neurophysiol 59:450–467.

Shalinsky MH, Magistretti J, Ma L, Alonso AA (2002) Muscarinic activation of a cation current and associated current noise in entorhinal-cortex layer-II neurons. J Neurophysiol 88:1197–1211.

Smiley JF, Morrell F, Mesulam MM (1997) Cholinergic synapses in human cerebral cortex: an ultrastructural study in serial sections. Exp Neurol 144:361–368.

Stutzmann GE, LaFerla FM, Parker I (2003) Ca^{2+} signaling in mouse cortical neurons studied by two-photon imaging and photoreleased inositol triphosphate. J Neurosci 23:758–765.

Turrini P, Casu MA, Wong TP, De Koninck Y, Ribeiro-da-Silva A, Cuello AC (2001) Cholinergic nerve terminals establish classical synapses in the rat cerebral cortex: synaptic pattern and age-related atrophy. Neuroscience 105:277–285.

Vinson PN, Justice Jr JB (1997) Effect of neostigmine on concentration and extraction fraction of acetylcholine using quantitative microdialysis. J Neurosci Methods 73:61–67.

Wang Z, McCormick DA (1993) Control of firing mode of corticotectal and corticopontine layer V burst-generating neurons by norepinephrine, acetylcholine, and 1S,3R-ACPD. J Neurosci 13:2199–2216.

Winkler J, Suhr ST, Gage FH, Thal LJ, Fisher LJ (1995) Essential role of neocortical acetylcholine in spatial memory. Nature 375:484–487.

Yamada S, Takechi H, Kanchiku I, Kita T, Kato N (2004) Small-conductance Ca^{2+}-dependent K^+ channels are the target of spike-induced Ca^{2+} release in a feedback regulation of pyramidal cell excitability. J Neurophysiol 91:2322–2329.

Yamamoto K, Hashimoto K, Nakano M, Shimohama S, Kato N (2002) A distinct form of calcium release down-regulates membrane excitability in neocortical pyramidal cells. Neuroscience 109:665–676.